Articles

Preparation, Characterization, DNA Binding, and *in Vitro* Cytotoxicity of the Enantiomers of the Platinum(II) Complexes *N*-Methyl-, *N*-Ethyl- and *N*,*N*-Dimethyl-(*R*)- and -(*S*)-3-aminohexahydroazepinedichloroplatinum(II)

Evonne M. Rezler,[†] Ronald R. Fenton,*[,†] Warren J. Esdale,[‡] Mark J. McKeage,[‡] Pamela J. Russell,[‡] and Trevor W. Hambley*[,†]

School of Chemistry, University of Sydney, NSW 2006, Australia, and Oncology Research Centre, Prince of Wales Hospital, NSW 2031, Australia

Received December 17, 1996[⊗]

A series of chiral diaminedichloroplatinum(II) complexes derived from [Pt(ahaz)Cl_2] (ahaz = 3-aminohexahydroazepine) have been synthesized and tested for cytotoxic activity. Novel synthetic pathways were developed to produce the structural derivatives of the ahaz ligand, with alkyl substituents on the exocyclic nitrogen atom. The platinum(II) complexes of these ligands were synthesized and characterized by NMR and CD spectroscopy, confirming isomeric and enantiomeric purity. The crystal structures of three of these complexes, [Pt(*S*-meahaz)Cl_2], [Pt(*R*-etahaz)Cl_2], and [Pt(*S*-dimeahaz)Cl_2] (meahaz = *N*-methylahaz, etahaz = *N*-ethylahaz, dimeahaz = *N*,*N*-dimethylahaz), have been determined to establish the orientation of the protons and alkyl substituents on the nitrogen donor atoms. *In vitro* assays of the cytotoxic activity of the complexes have revealed a significant and reproducible enantioselective trend with the *R*-enantiomers more active than the *S*-enantiomers in all cell lines. Increasing the steric bulk on the amine groups was found to have only a modest effect on activity. No enantioselectivity was observed in the binding of *R*- and *S*-[Pt(etahaz)Cl_2] to calf-thymus DNA.

Introduction

Platinum-based anti-cancer drugs such as *cisplatin* are believed to effect their cytotoxic action by forming one or more bifunctional adducts with DNA,[1−3] but it is still not known which of the adducts contribute to the cytotoxic activity of Pt(II) complexes. We have been using molecular modeling methods to design compounds that selectively form a subset of the adducts and so act as probes of the role of each adduct. Our approach to the investigation of the major adducts, intrastrand GpG and ApG, has been to use chiral compounds designed to bind enantioselectively at these sites.[4,5] The basis of this design is shown in Scheme 1. Our models reveal that when *cisplatin* forms GpG and ApG adducts, two hydrogen bonds can result, one to the phosphate group on the 5′ side of the adduct and the other to the O6 atom of the 3′ guanine. The energy contribution from the hydrogen bonds is probably not a major factor, but our studies suggest that replacement of the latter hydrogen bond, in particular, with an unfavorable interaction can influence the degree of binding at these sites.[6] Thus a pair of enantiomers, one having H atoms disposed appropriately for hydrogen bonding (Scheme 1a) and the other having bulky substituents disposed toward the hydrogen-bonding groups (Scheme 1b) could be expected to interact differently when forming bifunctional intrastrand adducts.

The difficulty faced in testing this hypothesis is the potential racemization of chiral centers on the coordinated amine. In order to overcome this, it is necessary to use a ligand framework that has inert chiral centers that impose the desired chirality at the nitrogen atoms. Our first attempt at this using a disubstituted 2,4-pentadiamine ligand was only partially successful because control over the chirality at the nitrogen atoms was not complete.[4] Consequently, we have turned to less flexible ligands and, for instance, have recently reported on the differential cytotoxicity and DNA binding of [Pt(*R*-ahaz)Cl_2] and [Pt(*S*-ahaz)Cl_2] (ahaz = 3-aminohexahydroazepine, Scheme 2, R′ = R″ = H).[5] The ahaz ligand has an endocyclic secondary amine and an exocyclic primary amine, with the carbon atom bonded to the exocyclic amine being chiral. Addition of

Scheme 1

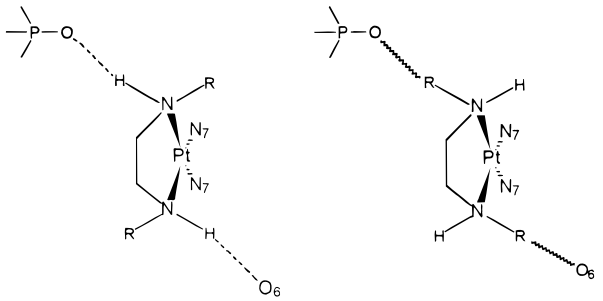

Scheme 2

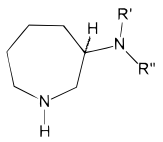

* Author to whom correspondence should be addressed. Fax: +61-2-9351-3329.
[†] University of Sydney.
[‡] Oncology Research Centre.
[⊗] Abstract published in *Advance ACS Abstracts,* October 1, 1997.

S0022-2623(96)00854-0 CCC: $14.00

a substituent to the primary amine would give a ligand with the features shown in Scheme 1. Upon coordination, a second chiral center on the exocyclic amine is generated. In the present paper we report the synthesis of two such ligands (meahaz = 3-(*N*-methylamino)-hexahydroazepine, Scheme 2, R′ = H, R″ = Me, and etahaz = 3-(*N*-ethylamino)hexahydroazepine, Scheme 2, R′ = H, R″ = Et) and their platinum complexes. We have also synthesized the ligand with two methyl substituents on the primary amine of ahaz (dimeahaz = 3-(*N*,*N*-dimethylamino)hexahydroazepine, Scheme 2, R′ = Me, R″ = Me, and its complex to assess the effect of increasing the steric bulk and removing the amine proton. The crystal structures of these three complexes and the *in vitro* cytotoxicities of the three pairs of enantiomers are also reported.

Experimental Section

Instrumental. The ^{1}H and ^{13}C NMR analyses were carried out on either a Bruker AMX 400 MHz spectrometer or a Bruker AC 200F spectrometer. The solvents were commercially obtained and were of 99.6% isotopic purity or better. The polarimetric studies of the ligands and their intermediates were carried out on an Optical Activity Polaar 2001 automatic polarimeter, using a 1 dm cell and were recorded at ambient temperature. The mass spectroscopic analysis of the ligands was carried out on a Kratos MS9 (updated to an MS50); ionization energy was achieved by physical electron impact at 70 eV. The samples were run on a direct insertion probe with a source temperature of 150−200 °C. The data collection system used was a Kratos DS90. The circular dichroism measurements for all the complexes were carried out on a JASCO J-710 spectropolarimeter equipped with J-700 software for Windows. The instrument was calibrated with camphor sulfonate (188.7 mdeg at λ_{max} 291.5 nm) prior to running the spectra. All spectra of the complexes were recorded using 10^{-3} M *N*,*N*-dimethylformamide (DMF) solutions, with a sensitivity setting of 50 mdeg and spectral band width at 1.0 nm, between 260 and 500 nm. Diffuse reflectance infrared Fourier transform spectra (DRIFTS) of the platinum complexes were collected on a Bio-Rad FTS-40 spectrophotometer equipped with Win-IR Windows based software. KBr was used for a background and as a matrix, over a range of 400−4000 cm^{-1}. All melting points were measured on a Gallenkamp model digital melting point apparatus and are reported uncorrected. The microanalysis of each complex was carried out by the National Analytical Laboratories Pty Ltd.

Resolution of Racemic α-Amino-ϵ-caprolactam (*rac*-amcap). The resolution of the precursor, *rac*-amcap (Sigma-Aldrich), was necessary as the *R*-enantiomer is not commercially available. The resolution procedure used was a modification of the method described by Boyle *et al*.[7] A vigorously stirred solution of dimethoxyethane (300 mL) and *rac*-amcap (51.2 g, 0.4 mol) was heated to 70 °C, and over a period of 10 min, (*S*)-2-oxopyrrolidin-5-carboxylic acid (L-PCA) (26.9 g, 0.21 mol) was added. The mixture was refluxed for 0.5 h, cooled to 30 °C, and then filtered. The yellowwhite filter cake was boiled in ethanol (500 mL), filtered, and washed with ethanol to give the white *S*-amcap.L-PCA salt (37.9 g). This was suspended in methanol (600 mL) and treated with concentrated hydrochloric acid (24.2 mL) to precipitate (*S*)-α-amino-ϵ-caprolactam as a white hydrochloride salt (*S*-amcap·HCl). The solid was filtered, washed with ethanol, and dried *in vacuo*: yield: 17.1 g, 67%; $[\alpha]_D$ −27.7° (c = 4, 1 M HCl).

The filtrate was condensed on a rotary evaporator to leave *R*-amcap·L-PCA as a dark yellow oil (22.40 g). This oil was dissolved in methanol (150 mL) and treated with concentrated hydrochloric acid (14.5 mL) to precipitate (*R*)-α-amino-ϵ-caprolactam as the hydrochloride salt (*R*-amcap·HCl). The solid was filtered, washed with a little ethanol followed by diethyl ether, and dried *in vacuo*: yield 11.51 g, 45%; $[\alpha]_D$ +26.8° (c = 4, 1 M HCl) (lit.[7] $[\alpha]_D$ +26.4°).

R-amcap·HCl (7.50 g, 0.05 mol) was dissolved in a minimum volume of water (30 mL) and shaken with sodium carbonate (2.50 g, 0.025 mol). Absolute ethanol (475 mL) was then added and the solvent removed by rotary evaporation to leave a yellow/white residue. More absolute ethanol (250 mL) was added to azeotropically remove any residual water present. The resulting solid, which consisted of sodium chloride and sodium carbonate, was filtered off, and the solvent was again removed by rotary evaporation. The product *R*-amcap was collected as a clear yellow oil: yield 7.00 g, ∼100%.

S-amcap·HCl was liberated as described above to produce *S*-amcap, again in almost quantitative yield. Both enantiomerically pure compounds were used as precursors in the syntheses of the following ligands.

Preparation of 3-(*N*-Methylamino)hexahydroazepine (meahaz). The synthesis of meahaz was adapted from the procedure published by Kashiwabara *et al*.[8] for the dimethylation of 1,2-cyclohexanediamine. The enantiomerically pure amcap·HCl (7.00 g, 0.046 mol) solid was added to an ice-cold, magnetically stirred solution of sodium hydroxide (5.60 g, 0.14 mol) in water (40 mL). A solution of ethyl chloroformate (3.7 mL, 0.046 mol) in benzene (20 mL) was added dropwise to the cooled mixture over a period of 1 h. The reaction mixture was allowed to stand at room temperature for 3 h, and then the crude product was extracted with dichloromethane (3 × 100 mL), dried over anhydrous sodium sulfate, and filtered. The solvent was removed from the filtrate by rotary evaporation, and the residual oil was then cooled in an acetone/ice bath to induce crystallization. The solid was washed with 60/90 petroleum ether to remove a soluble yellow impurity, leaving a pale-yellow solid: yield 7.00 g, 82%, based on the ethyl chloroformate amcap intermediate; MS *m*/*z* 200, calcd 200.

The (*R*)-ethyl chloroformate amcap intermediate (7.00 g, 0.035 mol) was added to sodium dried tetrahydrofuran (200 mL) and stirred. Freshly crushed lithium aluminum hydride (10.3 g) was slowly added to the cooled mixture, and the reaction mixture was allowed to warm to room temperature and was then refluxed for 48 h. Upon cooling, a solution of water (30 mL) in tetrahydrofuran (70 mL) was added dropwise to the reaction solution. The resultant mixture was gently refluxed for 0.5 h, and the solid was then removed by suction filtration and washed with boiling tetrahydrofuran (2 × 100 mL). The combined filtrates were condensed on a rotary evaporator, and benzene was used to azeotropically remove any residual water. The crude *R*-meahaz ligand was collected as a yellow oil: yield: 4.58 g, 92%. The ligand was further purified by vacuum distillation (Kugelrohr) at *ca*. 80 °C, 0.05 mmHg, to produce *R*-meahaz as a colorless oil: yield 3.32 g; MS *m*/*z* 128, calcd 128. NMR (solvent $CDCl_3$, ppm) 1.49 (m, 2H), 1.65 (m, 5H), 1.83 (m, 1H), 2.40 (s, 3H), 2.60 (m, 1H), 2.73 (q, 1H), 2.85 (m, 2H), 2.91 (dd, 1H), $[\alpha]_D$ +10.9 (c = 0.1, methanol). A similar procedure was followed to synthesize the *S*-meahaz ligand; the NMR spectrum of this compound was identical to that reported above for *R*-meahaz: yield: 7.51 g, 75%; distillation at *ca*. 80 °C, 0.05 mmHg; yield 6.52 g; MS *m*/*z* 128, calcd 128; $[\alpha]_D$ −11.0 (c = 0.1, methanol).

Preparation of 3-(*N*-Ethylamino)hexahydroazepine (etahaz). Acetic anhydride (40 mL, 0.36 mol) was slowly added to *R*-amcap (10 g, 0.078 mol), followed by 3 drops of pyridine. The mixture was stirred for 1 h and allowed to stand for a further 4 h, after which the solvent was removed by rotary evaporation. The crude product was broken up in ethyl acetate (20 mL), filtered, washed with ethyl acetate (2 × 10 mL), and air-dried. The white solid (*R*)-α-(acetylamino)-ϵ-caprolactam was collected at the pump: yield 9.00 g, 67%; mp 155−157 °C; $[\alpha]_D$ −12.27 (c = 1, methanol); MS *m*/*z* 170, calcd 170.

(*R*)-α-(Acetylamino)-ϵ-caprolactam (9.00 g, 0.053 mol) was added to sodium-dried tetrahydrofuran (250 mL) and stirred. Freshly crushed lithium aluminum hydride (31.0 g) was slowly added to the cooled mixture. The reaction mixture was allowed to reach room temperature and then refluxed for 48 h. The mixture was cooled, a solution of water (62 mL) in tetrahydrofuran (38 mL) was added dropwise, and the resultant mixture was gently refluxed for 0.5 h. The solid was removed by suction filtration and washed with boiling tet-

Table 1. Synthetic and Microanalytical Results

complex and molecular formula	yield (%)	calculated (%)			found (%)		
		C	H	N	C	H	N
[Pt(*R*-meahaz)Cl_2] $C_7H_{16}N_2Cl_2Pt$	58	21.33	4.09	7.11	21.3	4.2	6.9
[Pt(*S*-meahaz)Cl_2] $C_7H_{16}N_2Cl_2Pt$	63	21.33	4.09	7.11	21.3	4.2	6.9
[Pt(*R*-etahaz)Cl_2] $C_8H_{18}N_2Cl_2Pt$	58	23.54	4.44	6.86	23.5	4.8	6.6
[Pt(*S*-etahaz)Cl_2] $C_8H_{18}N_2Cl_2Pt$	45	23.54	4.44	6.86	23.2	4.2	6.6
[Pt(*R*-dimeahaz)Cl_2] $C_8H_{18}N_2Cl_2Pt$	69	23.54	4.44	6.86	23.7	4.6	6.7
[Pt(*S*-dimeahaz)Cl_2] $C_8H_{18}N_2Cl_2Pt$	62	23.54	4.44	6.86	23.1	4.4	6.4

rahydrofuran (3 × 100 mL). The combined filtrates were then condensed on a rotary evaporator and benzene used to azeotropically remove any remaining water. The crude *R*-etahaz ligand was a clear yellow oil: yield 5.88 g, 78%; MS *m*/*z* 142, calcd 142; NMR (solvent $CDCl_3$, ppm) 1.09 (t, 3H), 1.46 (br m, 2H), 1.68 (br m, 5H), 2.62 (q, 2H), 2.73 (m, 2H), 2.89 (m, 4H); $[\alpha]_D$ +9.8 (*c* = 0.1 methanol). *S*-etahaz was synthesized as described above, substituting *S*-amcap for *R*-amcap: yield 8.74 g, ~100%; $[\alpha]_D$ −10.0 (*c* = 0.1, methanol).

Preparation of 3-(*N*-Dimethylamino)hexahydroazepine (dimeahaz). The following procedure was based on the methods of Borch and Hassid[9] and Fenton *et al.*[10] A sample of *R*-amcap (7.00 g, 54.5 mmol) was dissolved in acetonitrile (300 mL), and aqueous formaldehyde (37 % v/v, 43.6 mL, 545 mmol) was added. Sodium cyanoborohydride (10.36 g, 164 mmol) was added to the mixture with stirring followed by glacial acetic acid (5.5 mL) added dropwise over 10 min. After the mixture was stirred for 2 h, more glacial acetic acid (5.5 mL) was added and the mixture was adjusted to approximately pH 7. After a further 0.5 h of stirring, the mixture was allowed to stand for 12 h at room temperature. The solvent was removed at reduced pressure, and potassium hydroxide (280 mL, 2M) was added to the residue until the pH was greater than 14. The organic compounds were extracted with dichloromethane (4 × 70 mL), combined, and dried over anhydrous sodium sulfate. Subsequent removal of the solvent on the rotary evaporator produced the crude *R*-dimeamcap, a pale-yellow oil, that was dried azeotropically with benzene: yield 7.63 g, 89%; MS *m*/*z* 156, calcd 156.

A sample of *R*-dimeamcap (7.63 g, 0.049 mol) was reduced to the *R*-dimeahaz ligand using lithium aluminum hydride in tetrahydrofuran, as described in the preceding methods: yield 4.50 g, 65%. The crude *R*-dimeahaz ligand was further purified by distillation at 100−125 °C, 0.05 mmHg, to give *R*-dimeahaz as a clear oil: yield 3.41 g; MS *m*/*z* 142, calcd 142; NMR (solvent $CDCl_3$, ppm) 1.42 (m, 1H), 1.72 (m, 6H), 2.25 (s, 6H), 2.35 (m, 1H), 2.74 (m, 1H), 2.85 (m, 4H); $[\alpha]_D$ +9.0 (*c* = 0.1 methanol). *S*-dimeahaz ligand was synthesized using the same procedure as for the *R*-dimeahaz ligand: yield 4.25 g, 57%. The crude *S*-dimeahaz was distilled at 100−125 °C, 0.05 mmHg: yield 3.12 g, 73%; MS *m*/*z* 142, calcd 142; $[\alpha]_D$ −9.3 (*c* = 0.1 methanol). The NMR spectrum of this ligand was identical to that reported above for *R*-dimeahaz.

Preparation of [Pt(L)Cl_2] Complexes (L = meahaz, etahaz, dimeahaz). [Pt(DMSO)$_2Cl_2$][11] (0.422 g, 1 mmol) was suspended in methanol (40 mL), and a solution of the diamine ligand, L (1 mmol), in methanol (20 mL) was added. The reaction mixture was stirred until all solids had dissolved and the solution was a clear pale-yellow color. The solvent was removed on a rotary evaporator at 40 °C. The resulting yellow residue was dissolved in water (20−30 mL) with excess lithium chloride (~0.5 g). The mixture was gently heated on a steam bath until the volume had been reduced to about 10 mL, and the solution was then left to stand at room temperature until the product crystallized as pale-yellow needles. The [Pt(L)Cl_2] complex was filtered, washed with a few drops of ice-cold water, ethanol, and ether, and air-dried. The yields obtained for the platinum complexes and the microanalytical results for each complex are presented in Table 1.

Crystallography. Crystals of [Pt(*S*-meahaz)Cl_2], [Pt(*R*-etahaz)Cl_2], and [Pt(*S*-dimeahaz)Cl_2], suitable for X-ray crystallography, were obtained by recrystallization of the complexes from hot DMF. The crystals were mounted, using glass fibers, on an Enraf-Nonius CAD4-F diffractometer equipped with a graphite monochromator. Cell constants were determined by least-squares fits to the setting angles values of 25 independent reflections, measured and refined on the diffractometer. The crystallographic data are summarized in Table 2. Lorentz, polarization, and analytical absorption corrections were applied using the teXsan crystallographic software package.[12] The structures were solved by direct methods using SHELXS-86,[13] and the solutions were extended by difference Fourier methods. Hydrogen atoms were included at calculated sites (C−H, N−H 0.95 Å) with isotropic thermal parameters based on those of the parent atoms, and all other atoms were refined anisotropically. The absolute configuration of each complex was confirmed by inverting all coordinates and repeating the final cycles of least squares refinement; the *R* values at convergence for the alternate configurations were 0.038, 0.023, and 0.041 for [Pt(*S*-meahaz)Cl_2], [Pt(*R*-etahaz)Cl_2], and [Pt(*S*-dimeahaz)Cl_2], respectively. Full-matrix least-squares methods were used to refine an overall scale factor and positional and thermal parameters. A $1/\sigma^2(F_o)$ weighting was used for all refinements. Neutral atom scattering factors were taken from Cromer and Waber.[14] Anomalous dispersion effects were included in F_c;[15] the values for $\Delta f'$ and $\Delta f''$ were those of Creagh and McAuley.[16] The values for the mass attenuation coefficients are those of Creagh and Hubbell.[17] All calculations were performed using the teXsan system,[12] and plots (Figures 1−3) were drawn using ORTEP.[18]

DNA Binding. Calf thymus DNA and Tris [tris(hydroxymethyl)aminomethane] were obtained from Sigma. The disodium salt of EDTA dihydrate was obtained from Merck. The 12−14 kDa dialysis membrane was purchased from Selby and was prepared by boiling in a solution containing 2% w/v

Table 2. Crystal Data

	[Pt(*S*-meahaz)Cl_2]	[Pt(*R*-etahaz)Cl_2]	[Pt(*S*-dimeahaz)Cl_2]
formula	$C_7H_{16}N_2Cl_2Pt$	$C_8H_{18}N_2Cl_2Pt$	$C_8H_{18}N_2Cl_2Pt$
fw	394.20	408.23	408.23
space group	$P2_12_12_1$	$P2_1$	$P2_12_12_1$
a, Å	8.660(3)	7.928(1)	8.367(2)
b, Å	10.722(4)	9.445(2)	9.935(4)
c, Å	11.986(4)	8.578(1)	28.479(5)
β, °		107.01(1)	
V, Å^3	1113.0(7)	614.3(2)	2367(1)
Z	4	2	8
T, °C	21	21	21
$d_{calcd,\ g\ cm^{-3}}$	2.352	2.212	2.291
λ(Mo Kα), Å	0.7107	0.7107	0.7107
μ(Mo Kα), mm^{-1}	12.99	11.77	12.21
R^a	0.024	0.014	0.028
$R_w{}^a$	0.021	0.013	0.023

[a] $R = \Sigma(||F_o| - |F_c||)/\Sigma|F_o|$, $R_w = (\Sigma w(|F_o| - |F_c|)^2/\Sigma w F_o^2)^{1/2}$.

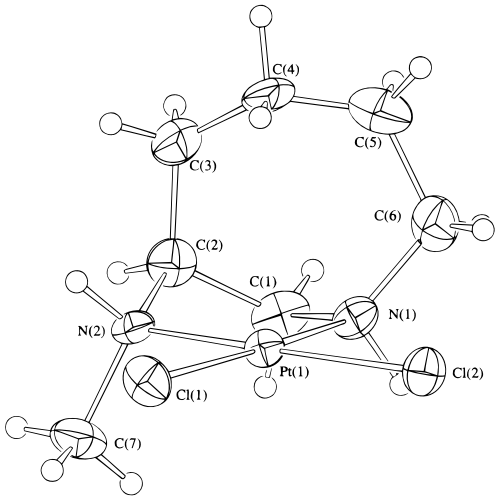

Figure 1. ORTEP plot for [Pt(*S*-meahaz)Cl_2].

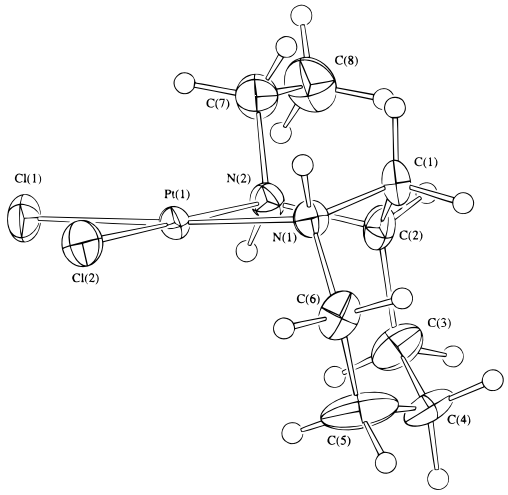

Figure 2. ORTEP plot for [Pt(*R*-etahaz)Cl_2].

sodium bicarbonate and 1 mM EDTA (pH 8.0) for 10 min, followed by rinsing thoroughly in distilled water and further boiling in 1 mM EDTA (pH 8.0) for 10 min. The membrane was cooled and stored in this solution at 4 °C. Dialysis was carried out using a BRL microdialysis system.

Graphite furnace atomic absorption spectroscopy (GFAAS) was performed on a Varian SpectrAA-20 absorption spectrometer equipped with a GTA-96 graphite tube atomizer and a PSC-56 autosampling system. UV absorbance was measured using a Hewlett-Packard diode array spectrometer.

The solutions of the platinum complexes were prepared immediately before use by dissolving in TE buffer (10 mM Tris, 0.1 mM EDTA, pH 7.4 adjusted with 10 M HCl) with heating and sonication and filtering through 0.22 μm cellulose acetate filters (MFS).

Calf thymus DNA (25 μg) was reacted with the platinum complexes in TE buffer in a total volume of 500 μL. The final platinum concentrations ranged from 0 to 150 μM, which corresponded to R_t (molar ratio of platinum added per nucleotide) of 0 and 0.98, respectively. The reaction mixtures were incubated at 37 °C for 24 h and were then stopped by the addition of 56 μL of 2 M NaCl. Any unbound platinum species were removed by dialysis against 3 L of TE buffer at 4 °C. The concentration of DNA in each reaction mixture was determined by measuring the absorbance at 260 nm (ξ_{260} {DNA}= 6600 M^{-1} cm^{-1}). The bound platinum concentration was analyzed using GFAAS. The results are presented as plots of the R_b (molar ratio of platinum bound to nucleotide) against the treated platinum concentrations in Figures 4−6. Cisplatin was included in the assays for comparison.

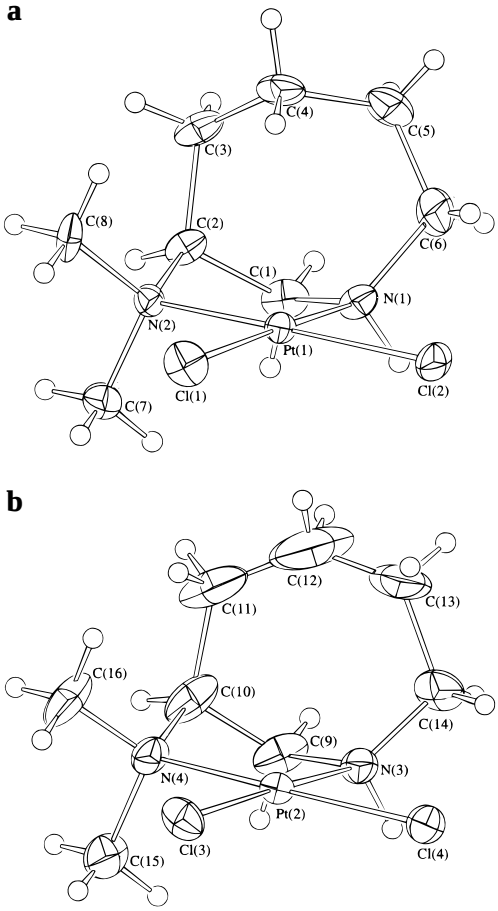

Figure 3. ORTEP plots of the two independent molecules of [Pt(*S*-dimeahaz)Cl_2].

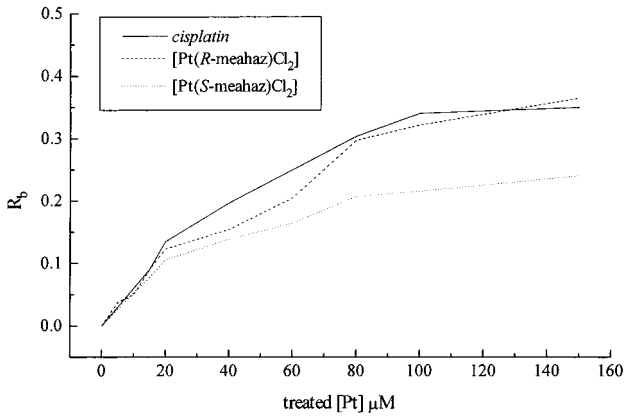

Figure 4. Concentration dependent DNA binding curves for cisplatin, [Pt(*R*-meahaz)Cl_2], and [Pt(*S*-meahaz)Cl_2].

Cytotoxicity Assays. The cell lines tested were human bladder tumor cells (UCRU BL13/0),[19] lung cancer cells (PC9 and PC9cisR), and prostate cancer cells (DU145). (PC9 is a cisplatin-sensitive cell line, and its resistant variant, PC9cisR, has decreased intracellular drug accumulation and elevated cellular glutathione levels.[20,21])

The tumor cells were grown as a monolayer culture in RPMI 1640 culture medium, which was supplemented with 10% foetal calf serum (FCS), penicillin, and streptomycin. Exponentially growing cells were maintained in a humidified incubator at 37 °C in an atmosphere of 7.5% CO_2, 5% O_2, and 85% N_2 until 60−80% confluence. The pH of the culture medium was monitored with phenol red and maintained at 7.2. For subsequent drug assays, the cell monolayers were washed with Hanks buffered saline and treated with trypsin−

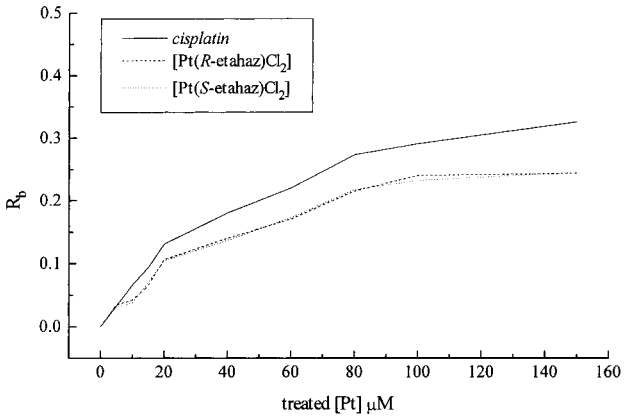

Figure 5. Concentration dependent DNA binding curves for cisplatin, [Pt(*R*-etahaz)Cl_2], and [Pt(*S*-etahaz)Cl_2].

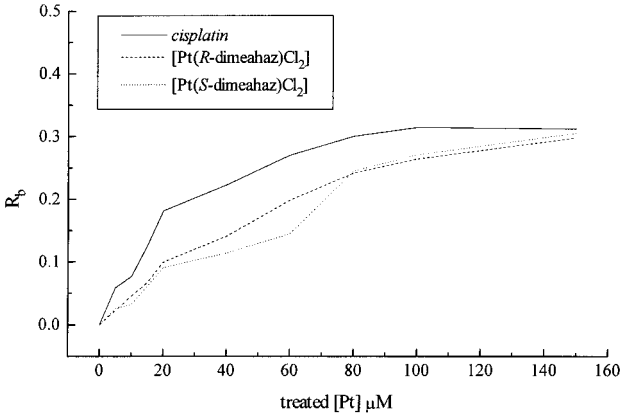

Figure 6. Concentration dependent DNA binding curves for cisplatin, [Pt(*R*-dimeahaz)Cl_2], and [Pt(*S*-dimeahaz)Cl_2].

EDTA to produce single-cell suspensions. The cells were seeded at a concentration of 5000 cells per well in 100 μL of tissue culture medium in 96-well microtitre plates and incubated at 37 °C for 24 h.

The platinum complexes were dissolved in 0.9% (w/v) NaCl saline with gentle heating and sonication immediately prior to use and filtered through 0.22 μm cellulose acetate filters. The solutions were diluted with the tissue culture medium, and 100 μL portions were added into the wells so that the final concentrations in the wells ranged from 0 to 200 μM. After 96 h of drug exposure at 37 °C, the drug-containing medium was removed and the cells were washed with 200 μL of warm phosphate-buffered saline (PBS) followed by 200 μL of warm tissue culture medium. The viable cell concentrations were determined using either the MTT assay or the SRB (sulforhodamine B) assay.

MTT Assay. This assay measures the cell viability by the activity of the mitochondrial succinate dehydrogenase.[22] MTT (3-(4,5-dimethylthiazol-2-yl)-2,5-diphenyltetrazolium bromide) in FCS-free RPMI tissue culture medium (1 mg mL^{-1}, 200 μL) was added into each well, and the plates were incubated at 37 °C for 4 h. After centrifugation and removal of the MTT solution, the formazan formed at the bottom of the wells was solubilized with 2-propanol (200 μL). The optical density at 570 nm for the solution in each well was determined using a Dynatech MR 5000 plate reader.

SRB Assay. In this assay, sulforhodamine B was used to stain the basic amino acids.[23] After the cells in each well were fixed with 200 μL of ice-cold 10% trichloroacetic acid for 30 min at 4 °C, the plates were washed five times with tap water. The fixed cells were stained with 100 μL of 0.4% sulforhodamine B dissolved in 1% acetic acid for 15 min at room temperature. The stain was then removed, and the plates were washed five times with 1% acetic acid and left to air dry overnight. Tris (10 mM, 100 μL) was added to solubilize the dye in each well, and the absorbance at 570 nm was read using a Dynatech MR 5000 plate reader.

In both assays, the percentage of viable cells was calculated by comparing the absorbance of the platinum-treated cells to that of the untreated controls. The cell viability for each concentration was an average value for four or six replicates. The IC_{50} values for the drugs (the concentration required to kill 50% of the cell population) was determined from the dose response curves.

Results and Discussion

Syntheses. It is imperative that these complexes be of high enantiomeric and chemical purity for them to be meaningful probes of Pt/DNA interactions. The *rac*-amcap precursor was successfully resolved by the formation of the two diastereomeric carboxylate salts and separation by virtue of their differing solubilities in dimethoxyethane. The resultant carboxylic acid salts were then converted to their respective enantiomers as amcap·HCl, and enantiomeric purity was confirmed by polarimetry. Subsequent reactions, on the resolved amcap precursor do not involve the chiral carbon atom. The ligands and platinum complexes were confirmed to be enantiomerically and chemically pure by CD and NMR spectroscopies and polarimetry.

The meahaz Ligand. The synthesis of the meahaz ligand posed some problems as other methods of methylation failed to singly methylate the exocyclic primary nitrogen atom, resulting instead in a mixture of mono- and dimethylated products. The successful synthesis of meahaz outlined in Scheme 3a involved the formation of an ester intermediate which was cleaved during the reduction with lithium aluminum hydride in THF. It is important to note that only the primary exocyclic nitrogen atom was methylated, and no reaction occurred on the amide nitrogen.

The etahaz Ligand. The enantiomerically pure ampcap precursor was acetylated with acetic anhydride and reduced to give etahaz (Scheme 3b). The alkylation of only the exocyclic nitrogen occurred because of the protection offered to the endocyclic nitrogen by the amide group. Similarly, in the process of acetylation, once an amide group forms, no further reaction takes place at the protected nitrogen, and reduction with lithium aluminum hydride produced the monoethylated product in high yield and purity.

The dimeahaz Ligand. The methylation and reduction processes used to synthesize dimeahaz are shown in Scheme 3c. The dimethylation of amcap proceeds through the formation of unstable imine intermediates, and the mild reducing agent,[24] sodium cyanoborohydride, was used successfully to reduce the imines to the amines *in situ*. The *N*,*N*-dimethyldiamine ligand was isolated, after workup, in high yield.

Characterization of the Platinum Complexes. The complexes were characterized by ^1H and ^{13}C NMR and CD spectra. In all cases the solvent used for these analyses was DMF (for CD spectra) or DMF-d_7. The DMF signals in the ^1H NMR spectra, due to the presence of an isotropic impurity, appear at 2.79, 2.94, and 7.90 ppm; in the ^{13}C NMR spectra two multiplets appear at 30 and 35 ppm. These resonances due to these impurities were used as internal calibrants. DMF was chosen as the solvent since all the complexes are soluble in DMF, and it was found that the chloride ligands did not exchange with DMF.

Scheme 3

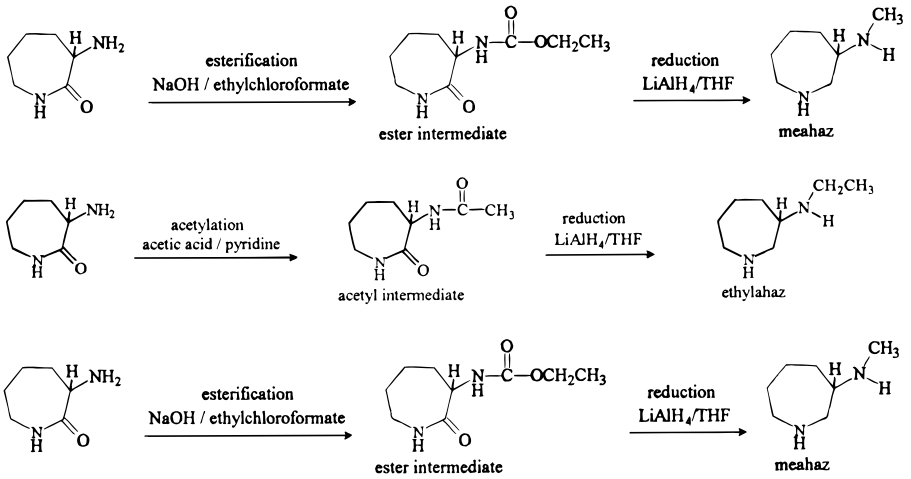

In the ^{1}H NMR spectra the H(amine) peaks for the endocyclic nitrogen were consistently located at 6.6−6.7 ppm which was approximately 1 ppm downfield from that of the excocyclic H(amine) atom due to deshielding effects. [Pt(ahaz)Cl_2] has two exocyclic amine proton signals, while [Pt(meahaz)Cl_2] and [Pt(etahaz)Cl_2] have one. The dimethylplatinum complex has only one protonated nitrogen atom in its structure as the substituted nitrogen has two methyl groups attached. The upfield section of the spectra is complex and difficult to interpret due to the interference of the large DMF solvent signals. The ^{1}H NMR spectra confirm that the exocyclic nitrogen atoms of the ligands had the attached substituent(s).

From the ^{13}C NMR spectra it is evident that only one diastereomer is present for each of [Pt(meahaz)Cl_2] and [Pt(etahaz)Cl_2], unless isomerization is taking place more rapidly than the NMR time scale, but this is highly unlikely. The number of carbon atoms in each complex was in accord with the number of peaks present in the spectra. DEPT spectra were collected to identify the different types of environment of the carbon atoms. The CD spectra of the complexes in DMF solvent were obtained and confirm the enantiomeric purity of the complexes. The three sets of enantiomers have qualitatively the same shape with bands in approximately the same positions. Since only the substituents on one nitrogen atom in each complex vary, the similarity between the spectra of the different complexes is to be expected.

Crystallography. The crystal structures of [Pt(*S*-meahaz)Cl_2], [Pt(*R*-etahaz)Cl_2] and [Pt(*S*-dimeahaz)Cl_2] were determined, and the ORTEP[18] plots are shown in Figures 1−3. The structural features common to all complexes are the square planar co-ordination around Pt(II) with *cis* chloro ligands and nitrogen donor atoms. The chloro ligands do not deviate significantly from the least-squares planes through the Pt and donor atoms. However, the nitrogen donor atoms deviate significantly from the square planar arrangement probably due to the steric demands of the ahaz ligand. The Pt−Cl bonds are approximately the same length in all structures and range from 2.297(1) to 2.320(1) Å. In all cases, the endocyclic nitrogen has the longest Pt−N bond length although this is not so in the parent complex [Pt(*S*-ahaz)Cl_2].[4] [Pt(*S*-dimeahaz)Cl_2] has two independent molecules in the asymmetric unit. Hydrogen bonding between a chloro ligand of one molecule and a H(amine) of the other molecule leads to weakly coupled dimers.

The chiralities of the complexes were confirmed to be as expected by inverting the coordinates and repeating the final cycles of refinement. The chiralities of both endocyclic and exocyclic amine ligands are both opposite to that of the chiral carbon atom of the ligand. In both [Pt(*S*-meahaz)Cl_2] and [Pt(*R*-etahaz)Cl_2] the alkyl substituent on the exocyclic nitrogen atom is, as anticipated, disposed away from the ahaz ring because of steric interactions. This results in the H(amine) atoms lying on opposite sides of the coordination plane as required by the design philosophy.

Large thermal ellipsoids for the C atoms in the seven-membered ahaz ring indicating either static or dynamic disorder were observed in some cases. The seven-membered ring commonly adopts one of two conformations that primarily differ in the disposition of the C(4) atom, toward or away from the Pt atom. Two C(4) positions of approximately equal occupancy were found in [Pt(*R*-etahaz)Cl_2]; in [Pt(*S*-meahaz)Cl_2] the ratio was more skewed toward one carbon position; and the two different conformations were observed in the two independent molecules of [Pt(*S*-dimeahaz)Cl_2].

Concentration Dependent DNA Binding Study. A concentration dependent study of the binding of cisplatin and the enantiomers of [Pt(meahaz)Cl_2], [Pt(etahaz)Cl_2], and [Pt(dimeahaz)Cl_2] to DNA was carried out. The moles of Pt bound per nucleotide of calf thymus DNA (R_b) versus the amount of the platinum complex added is plotted in Figures 4−6. The bound platinum is greatest for cisplatin at each level of treated platinum. This is not surprising given the greater steric bulk of the other complexes, but it may also be due to chemical differences. There is also no discernible difference in the binding results for the two enantiomers of the platinum complexes, with the possible exception of [Pt(meahaz)Cl_2], probably because the measurements encompass both bifunctional and monofunctional modes of binding and enantioselective differences are more likely to be observed for the bifunctional adducts. Surprisingly, the increased bulk of the [Pt(dimeahaz)-Cl_2] complex does not substantially influence the extent of DNA binding.

***In Vitro* Cytotoxicity Studies.** Results of the *in vitro* assays are presented in Table 3. In all cases the complexes with additional substituents on the primary

Table 3. IC_{50} Values

drug	mean IC_{50} (standard error)			
	BL13/0	PC9	PC9-cisR	DU145
cisplatin	1.9(0.5)	1.4(0.2)	11.7(3.1)	1.8(0.8)
[Pt(*R*-ahaz)Cl_2]	1.3(0.2)	5.9(0.1)	16.0(1.0)	2.9(0.1)
[Pt(*S*-ahaz)Cl_2]	2.0(0.2)	3.0(0.1)	15.3(1.3)	3.4(0.3)
[Pt(*R*-meahaz)Cl_2]	7.3(1.3)	13.3(1.9)	19.0(1.2)	6.7(1.3)
[Pt(*S*-meahaz)Cl_2]	11.7(1.6)	13.7(1.2)	38.3(8.0)	10.1(1.7)
[Pt(*R*-etahaz)Cl_2]	7.4(1.1)	20(3.5)	44(4.4)	9.5(0.9)
[Pt(*S*-etahaz)Cl_2]	19(2.1)	31(4)	79.7(8.5)	21.3(2.4)
[Pt(*R*-dimeahaz)Cl_2]	7.7(2.1)	13.5(3.4)	29.3(1.5)	7.3(0.2)
[Pt(*S*-dimeahaz)Cl_2]	10.2(1.4)	11.8(2.6)	28.7(2.2)	11.5(0.8)

amine are significantly less active than either cisplatin or the parent complexes [Pt(*R*-ahaz)Cl_2] and [Pt(*S*-ahaz)Cl_2]. The enantioselectivity is in line with but more pronounced than that previously reported for the parent complexes with, in nearly all cases, the *R* enantiomer being more active than the *S*. The enantioselectivity is greatest for the BL13/0 and DU145 cell lines and for [Pt(etahaz)Cl_2] where it is between 2:1 and 3:1. In the PC9 cell line the activity is lower than in either BL13/0 or DU145 and enantioselectivity is only observed for [Pt(etahaz)Cl_2]. In PC9-cisR, a cisplatin resistant variant of PC9, they are a factor of 2−3 times less active indicating some but not complete cross resistance, and interestingly, greater enantioselectivity is observed than in the resistant cell line. The resistance mechanism in PC9cisR is predominantly transport inhibition,[20,21] so the increased enantioselectivity in the resistant line might arise from differential uptake. However, resistance is usually multifactorial, and other factors such as intracellular deactivation and differential repair may play a role. Somewhat surprising is the observation that the [Pt(dimeahaz)Cl_2] enantiomers are no less active than those of [Pt(meahaz)Cl_2] and [Pt(etahaz)-Cl_2] complexes. On the basis of previous structure−activity models and our molecular models, we anticipated that replacement of both H(amine) atoms on the primary amine with alkyl groups would strongly inhibit binding to DNA and therefore inhibit activity. However, this result is in accord with DNA binding studies which showed that the increased bulk of [Pt(dimeahaz)Cl_2] did not influence the extent of binding.

Conclusions

Our primary goal in this study was to prepare and test pairs of enantiomerically related platinum complexes in which each amine group has only one hydrogen atom, and these H(amine) atoms are disposed toward opposite sides of the coordination plane. A series of substituted enantiomerically pure ligands derived from ahaz was synthesized and sucessfully complexed to platinum. Structural characterization of [Pt(*S*-meahaz)-Cl_2] and [Pt(*R*-etahaz)Cl_2] confirmed that the design goal of *trans* H(amine) atoms was achieved, and NMR studies showed that this arrangement overwhelmingly predominated in solution. Thus, on the basis of the interactions shown in Scheme 1, we expect that the *S* enantiomers of these complexes would readily form the bifunctional intrastrand adduct, but the *R* enantiomer would be less likely to do so. Since it is these adducts that are believed to be responsible for the majority of the cytotoxic activity of cisplatin and its close analogues,[1−3] we would expect the *S* enantiomer to be the more active.

Measurement of the DNA binding of the three pairs of enantiomers showed that all bound slightly less to DNA than does cisplatin, again a not unexpected result given the greater steric bulk. In the case of [Pt(etahaz)-Cl_2] and [Pt(dimeahaz)Cl_2] there is no difference in the DNA binding of the two enantiomers, and in the case of [Pt(meahaz)Cl_2] the *R* enantiomer may be marginally better at binding to DNA at high concentrations. Thus, we can conclude that neither steric bulk nor the chirality of the ligands exerts a substantial influence on the total DNA binding. These experiments do not distinguish between monofunctional and bifunctional adducts, and it is likely that greater differences will be observed in the extent of bifunctional adduct formation as is the case for the enantiomers of the parent complex [Pt(ahaz)-Cl_2].[5,25]

[Pt(meahaz)Cl_2] and [Pt(etahaz)Cl_2] had similar but moderate *in vitro* cytotoxicity against a number of cell lines and were about 5−6 times less active than the parent and [Pt(*R*- and *S*-ahaz)Cl_2] complexes or cisplatin. The moderate activity is consistent with the view that the presence of one H atom on each amine is sufficient for activity to be observed, and the reduced activity compared to the ahaz complexes is not suprising given the increased steric bulk of the substituents added to the primary amine. Replacement of both H atoms on the primary amine of [Pt(ahaz)Cl_2] with methyl groups, producing the [Pt(dimeahaz)Cl_2] complexes, was expected to substantially decrease their cytotoxicity relative to that of the other complexes. However, this was not the case with activities almost indistinguishable from those of the [Pt(meahaz)Cl_2] and [Pt(etahaz)Cl_2] complexes being observed in all cell lines. Thus, the notion that one H atom on each amine group is an essential requirement for cytotoxic activity needs to be questioned and investigated further.

Enantioselectivity similar to that of the parent complexes was observed in the cytoxicity experiments with, in nearly all cases, the *R* enantiomer being more active than the *S*. In some cases the *R* enantiomer is up to 3 times more active, but in others the differences in activity are of marginal signficance. We consider it noteworthy that the same enantiomer is the more active, particularly against the BL13 and DU145 cell lines, for all complexes. We had anticipated that higher levels of enantioselectivity might be observed if formation of the bifunctional intrastrand adducts was substantially influenced by the disposition of the H(amine) atoms, but we had predicted that it was the *S* enantiomer that would be the more active (see Scheme 1). In the case of the parent complex [Pt(ahaz)Cl_2], we have shown that, as expected, the *S* enantiomer forms more bifunctional adducts that the *R*.[25] Thus, the expected correlation between the extent of bifunctional adduct formation and cytoxicity is not observed. It is probable therefore, that a number of other factors, including cell uptake for example, contribute significantly to the enantioselectivity observed in the cytotoxicity. It is anticipated that the greater steric bulk of the present complexes will lead to even greater enantioselective differences in the tendency to form bifunctional adducts, and work is underway to investigate the DNA binding in more detail. We are also using these pairs of enantiomers in an attempt to establish what role other factors play in contributing to the cytotoxicity.

Acknowledgment. The support of the Sydney University Cancer Research Fund, the University of Sydney Research Grants Scheme, and the Australian Research Council is gratefully acknowledged.

Supporting Information Available: Tables of crystal data, positional and thermal parameters, bond lengths and angles, torsion angles, and least-squares planes (12 pages). Ordering information is given on any current masthead page.

References

(1) Pinto, A. L.; Lippard, S. J. Binding of the antitumor drug *cis*-diamminedichloroplatinum(II) (*cisplatin*) to DNA. *Biochem. Biophys. Acta* **1985**, *780*, 167−180.
(2) van der Veer J. L.; Reedijk J. Investigating antitumour drug mechanisms. *Chem. Br.* **1988**, *24*, 775−780.
(3) Sheibani, N.; Jennerwein, M. M.; Eastman, A. DNA repair in cells sensitive and resistant to *cis*-diamminedichloroplatinum-(II): Host cell reactivation of damaged plasmid DNA. *Biochemistry* **1989**, *28*, 3120−3124.
(4) Vickery, K.; Bonin, A. M.; Fenton, R. R.; O'Mara, S.; Russell, P. J.; Webster, L. K.; Hambley, T. W. The preparation, characterization, cytotoxicity and mutagenicity of a pair of enantiomeric platinum(II) complexes with the potential to bind enantioselectively to DNA. *J. Med. Chem.* **1993**, *36*, 3663−3668.
(5) Fenton, R. R.; Er, H. M.; O'Mara, S.; Russell, P. J.; Hambley, T. W. Preparation, DNA binding and *in vitro* cytotoxicity of a pair of enantiomeric platinum(II) complexes, (*R*)- and (*S*)-3-aminohexahydroazepine-dichloroplatinum(II). Crystal structure of the (*S*)-enantiomer. *J. Med. Chem* **1997**, *40*, 1090−1098.
(6) Hambley, T. W. A molecular mechanics analysis of the stereochemical factors influencing monofunctional and bifunctional binding of cis-diamminedichloroplatinum(II) to adenine and guanine nucleobases in the sequences d(GpApGpG):d(CpCpTpC) and d(GpGpApG):d(CpTpCpC) of A- and B-DNA. *Inorg. Chem.* **1991**, *30*, 937−942.
(7) Boyle, W. J.; Sifniades, S.; Van Peppen, J. F. Asymmetric transformation of α-amino-ϵ-caprolactam, a lysine precursor. *J. Org. Chem.* **1979**, *44*, 4841−4847.
(8) Kashiwabara, K.; Hanaki, K.; Kujita, J. Chiral recognition in catalytic hydrogenation of α-acylaminoacrylic acids by cationic rhodium(I) complexes of chiral aminophosphines derived from (*R*,*R*)-1,2-cyclohexanediamine or (*R*)-1,2-propanediamine. *Bull. Chem. Soc. Jpn.* **1980**, *53*, 2275−2280.
(9) Borch, R. F.; Hassid, A. I. A new method for the methylation of amines. *J. Org. Chem.* **1972**, *37*, 1673−1674.
(10) Fenton, R. R.; Stephens, F. S.; Vagg, R. S.; Williams, P. A. Chiral metal complexes 36. Stereoselectivity enhanced by *N*,*N*'-dimethylation of a chiral N_4 tetradentate, including the crystal structure of Δ-α_1,α_2-{[(*N*,*N*'-dimethyl-3*R*-methyl-1,6-di(2-pyridyl)-2,5-diazahexane)(*S*-alaninato)]-cobalt(III)} perchlorate. *Inorg. Chim. Acta* **1992**, *201*, 157−164.
(11) Price, J. H.; Williamson, A. N.; Schramm R. F.; Wayland, B. B. Palladium(II) and platinum(II) alkyl sulfoxide complexes. Examples of sulfur-bonded, mixed sulfur- and oxygen-bonded, and totally oxygen-bonded complexes. *Inorg. Chem.* **1972**, *11*, 1280−1284.
(12) TeXsan, Crystal Structure Analysis Package, Molecular Structure Corporation (1985 and 1992).
(13) Sheldrick, G. M. SHELXS-86, In *Crystallographic Computing 3*; (Sheldrick, G. M., Krüger, C., Goddard, R., Eds.; Oxford Univ. Press: Oxford, 1995; pp 175−189.
(14) Cromer D. T. J.; Waber, T. *International Tables for X-ray Crystallography*; Kynoch Press: Birmingham, 1974; Vol. 4.
(15) Ibers, J. A.; Hamilton, W. C. *Acta Crystallogr.* **1964**, *17*, 781.
(16) Creagh D. C.; McAuley, W. J. *International Tables for Crystallography*; Wilson, A. J. C., Ed.; Kluwer Academic Publishers: Boston, 1992; Vol. C, Table 4.2.6.8, pp 219−222.
(17) Creagh D. C.; Hubbell, J. H. *International Tables for Crystallography*; Wilson, A. J. C., Ed.; Kluwer Academic Publishers: Boston, 1992; Vol. C, Table 4.2.4.3, pp 200−206.
(18) Johnson, C. K. *ORTEP, A Thermal Ellipsoid Plotting Program*; Oak Ridge National Laboratories: Oak Ridge, 1965.
(19) Russell, P. J.; Wass, J.; Lukeis, R.; Garson, M.; Jelbart, M.; Wills, E.; Phillips, J.; Brown, J.; Carrington, N.; Vincent, P.; Raghavan, D. Chracterization of cell lines derived from a multiply aneuploid human bladder transitional-cell carcinoma UCRU-BL-13. *Int. J. Cancer* **1989**, *44*, 276−285.
(20) Fujiwara, Y.; Sugimoto, Y.; Kasahara, K.; Bungo, M.; Yamakido, M.; Tew, K. D.; Saijo, N. Determinants of drug response in a cisplatin-resistant human lung cancer cell line. *Jpn. J. Cancer* **1990**, *81*, 527−535.
(21) Morikage, T.; Ogmori, T.; Nishio, K.; Fujiwara, Y.; Takeda, Y.; Saijo, N. Modulation of cisplatin sensitivity and accumulation by amphotericin B in cisplatin-resistant human lung cancer cell lines. *Cancer Res.* **1993**, *53*, 3302−3307.
(22) Mosmann, T. Rapid colorimetric assay for cellular growth and survival. Application to proliferation and cytotoxicity assays. *Immunol. Methods* **1983,** *65*, 55−64.
(23) Skehan, P.; Storeng, R.; Scudiero, D.; Monks, A.; McMahon, J.; Vistica, D.; Warren, J. T.; Bokesh, H.; Kenney, S.; Boyd, M. R. New colorimetric cytotoxicity assay for anticancer-drug screening. *J. Natl. Cancer Inst.* **1990**, *82*, 1107−1112.
(24) March, J. *Advanced Organic Chemistry: Reactions, Mechanisms, and Structure*; 4th ed.; John Wiley and Sons: New York, 1992.
(25) Er, H. M. Chiral Probes of Pt/DNA Interactions, Ph.D. Thesis, University of Sydney, 1996.

JM960854N